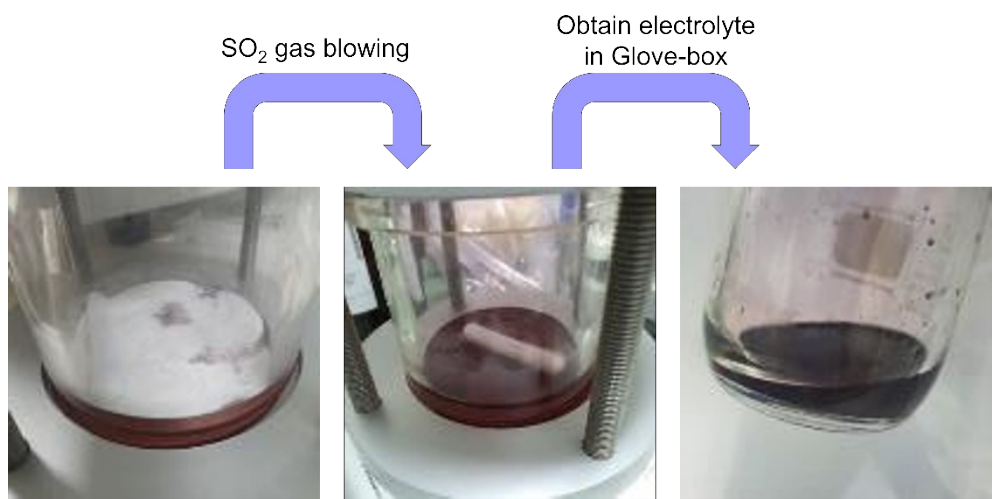
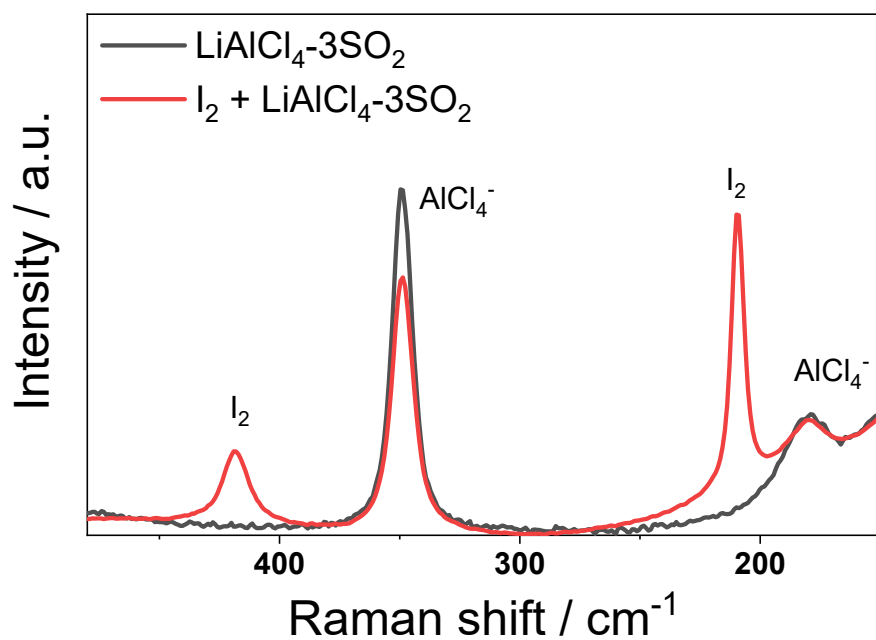


**Supplementary Information**

Iodine-Driven Artificial SEI layer for High Performance Lithium Metal Batteries in SO<sub>2</sub>-based Electrolyte



**Fig. S1.** Digital photographs of synthesis process for I<sub>2</sub>-containing LiAlCl<sub>4</sub>-3SO<sub>2</sub> electrolyte.



**Fig. S2.** Raman spectra of LiAlCl<sub>4</sub>-3SO<sub>2</sub> and I<sub>2</sub>-containing LiAlCl<sub>4</sub>-3SO<sub>2</sub> electrolytes.

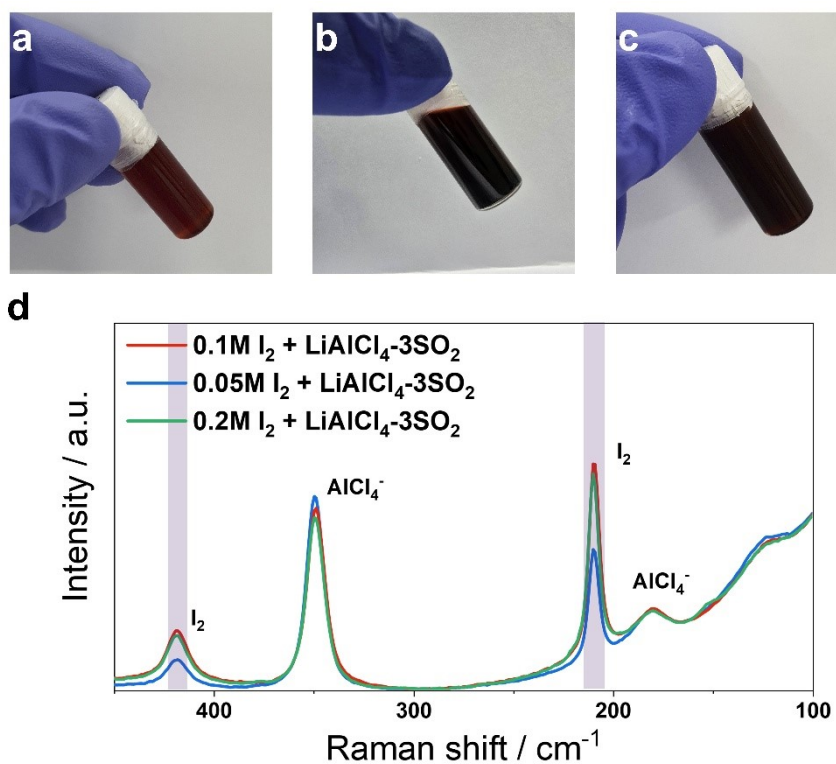


**Fig. S3.** (a–c) Comparison of digital photographs of iodine-containing LiAlCl<sub>4</sub>–3SO<sub>4</sub> electrolytes with different LiI levels: (a) 0.05M (light purple), (b) 0.10M (dark wine), and (c) 0.20M (dark wine; similar color to 0.10M). (d) Normalized Raman spectra of the corresponding electrolytes.

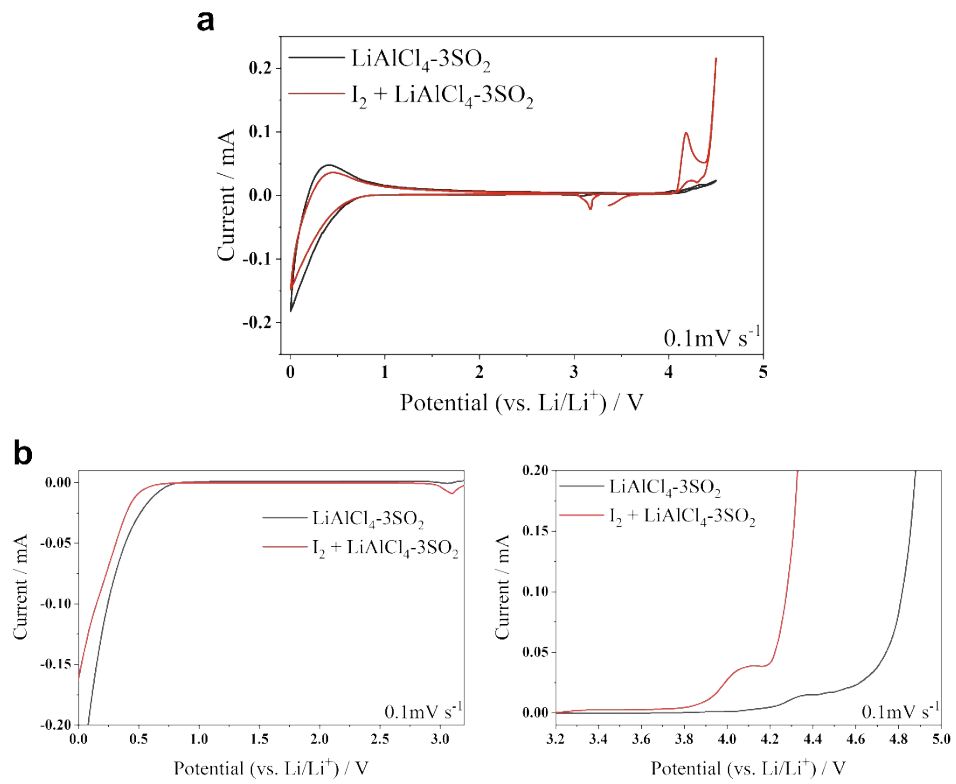


**Fig. S4.** (a) Cyclic voltammetry (CV) and (b) linear sweep voltammetry (LSV) of  $\text{LiAlCl}_4\text{-3SO}_2$  and  $\text{I}_2$ -added  $\text{LiAlCl}_4\text{-3SO}_2$  electrolytes.

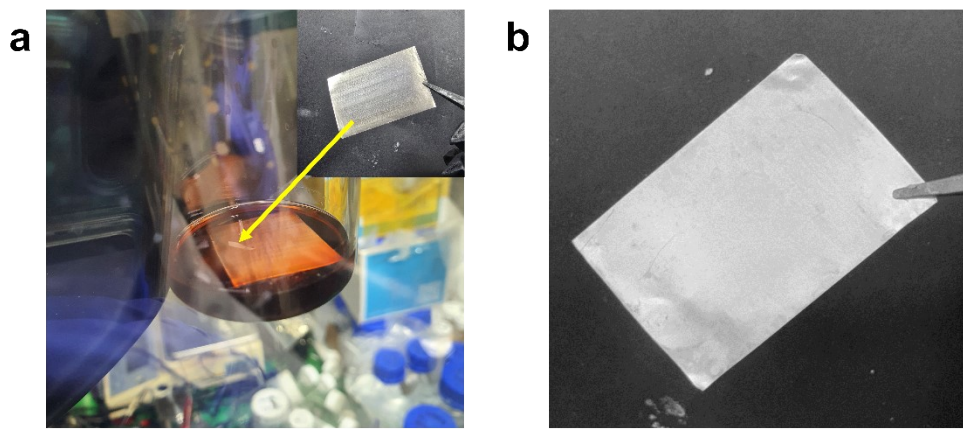


**Fig. S5.** (a) Digital photograph showing dipping process of pristine lithium metal (inset) and (b) lithium metal after the dipping process in  $I_2$ -containing  $LiAlCl_4\text{-}3SO_4$ .

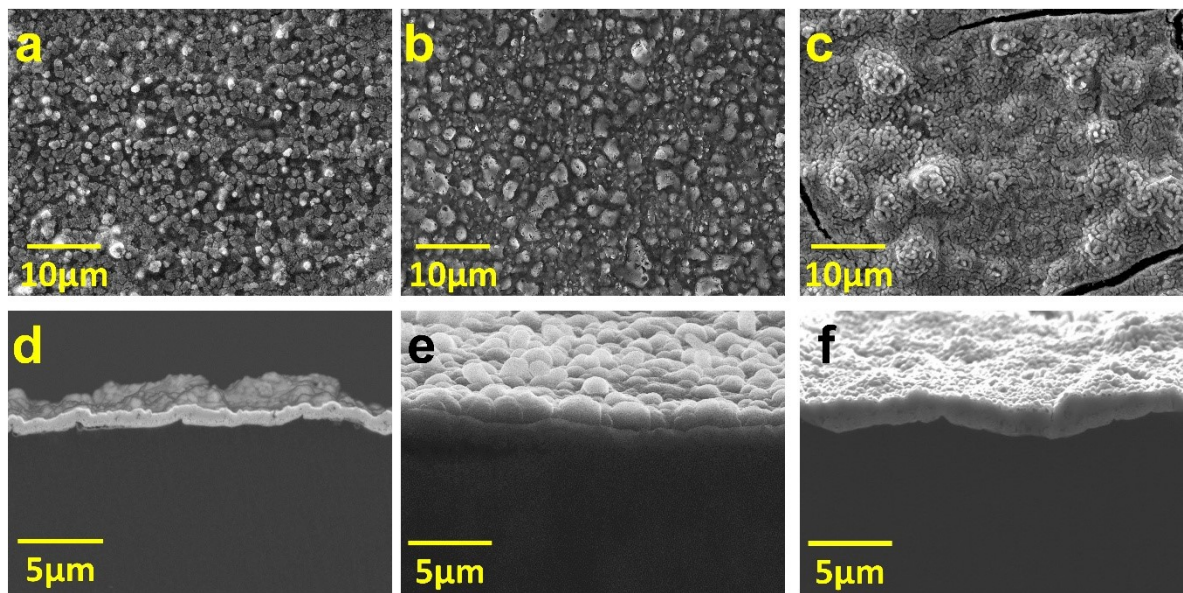


**Fig. S6.** Top-view SEM images of lithium metal after dipping in iodine-containing  $\text{LiAlCl}_4\text{--3SO}_2$  electrolytes with different  $\text{LiI}$  levels: (a) 0.05M, (b) 0.10M, and (c) 0.20M. Cross-sectional SEM images of the corresponding dipped lithium electrodes: (d) 0.05M, (e) 0.10M, and (f) 0.20M.

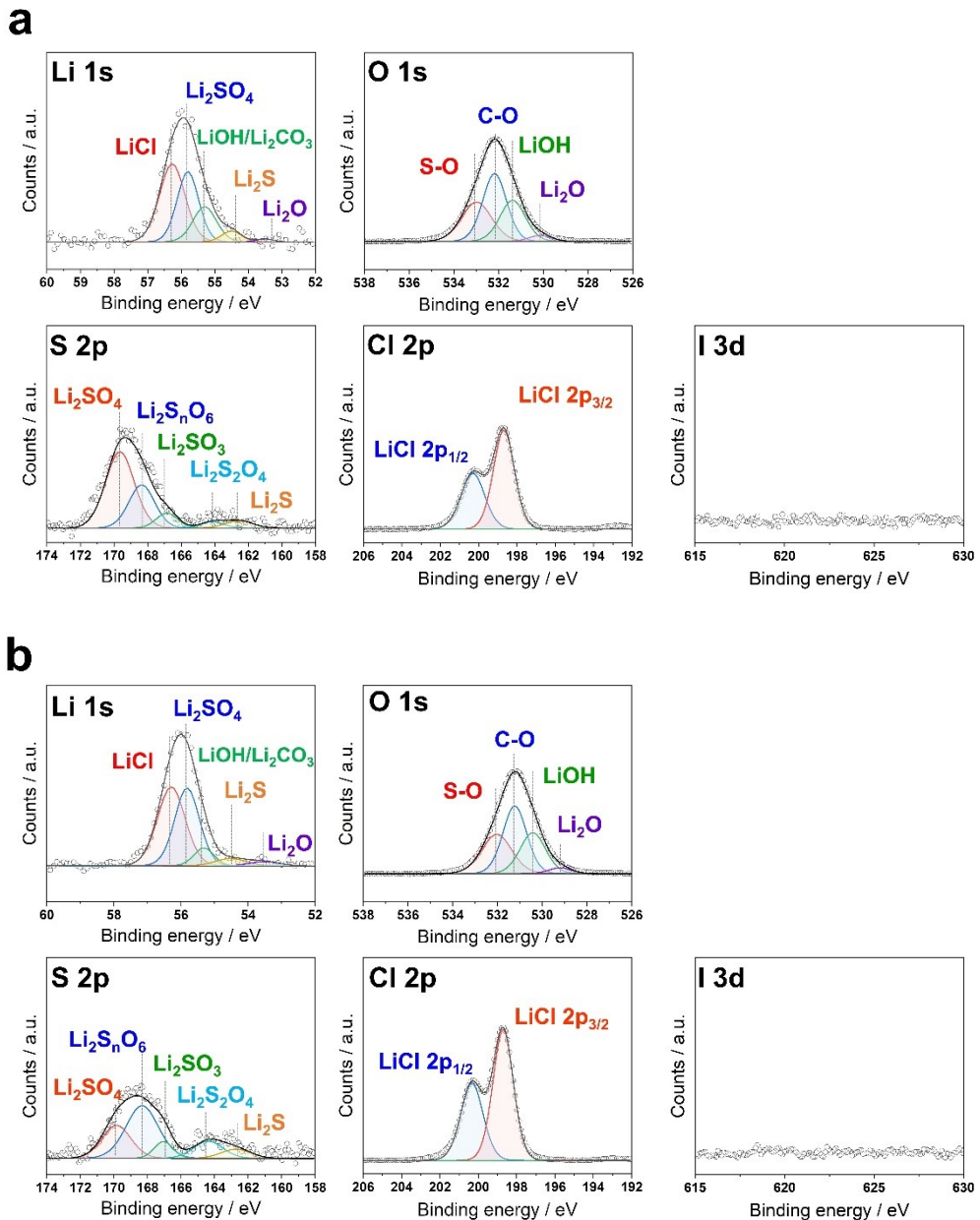


**Fig. S7.** XPS spectra (Li 1s, O 1s, S 2p, Cl 2p, and I 3d regions) of lithium electrodes after dipping in iodine-containing  $\text{LiAlCl}_4\text{--3SO}_2$  electrolytes with different  $\text{LiI}$  levels: (a) 0.05M and (b) 0.20M.

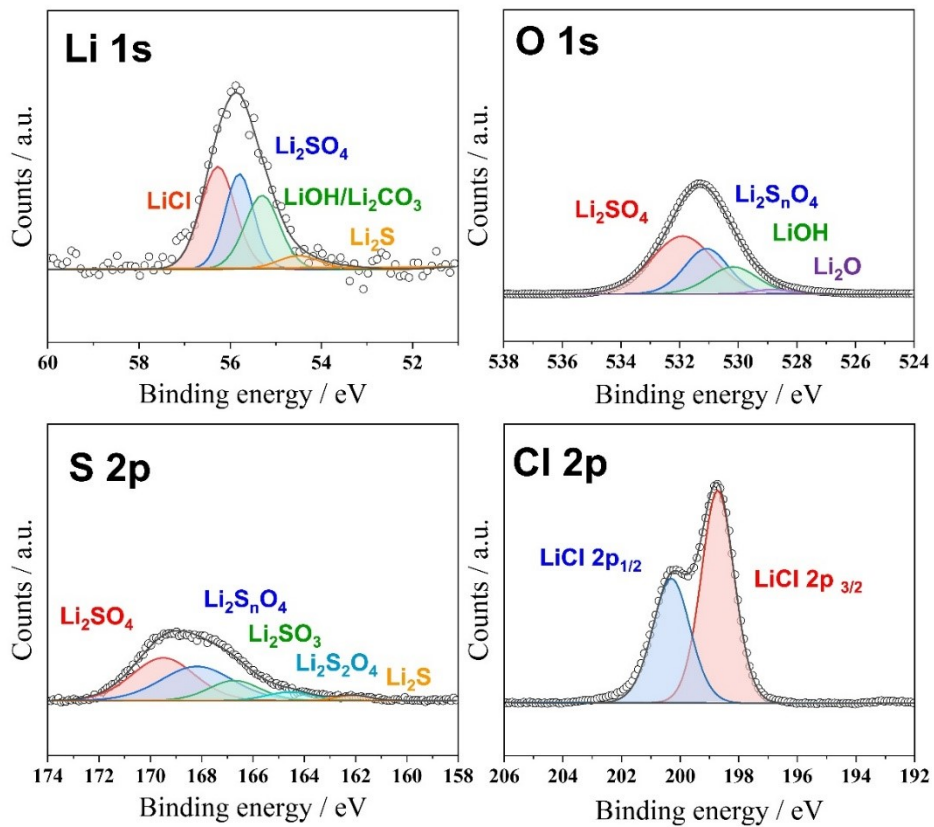


**Fig. S8.** Surface XPS spectra of Li 1s, O 1s, S 2p, and Cl 2p, at lithium metal surface after dipping with  $\text{LiAlCl}_4\text{-3SO}_2$  electrolyte.

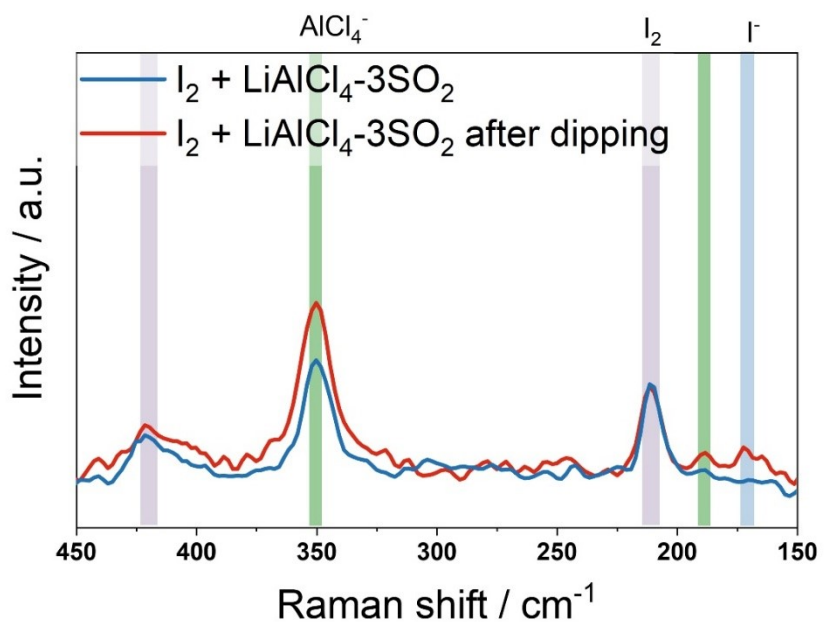


**Fig. S9.** Ex situ Raman spectra of the  $I_2$ –Li–SO<sub>4</sub> electrolyte before and after lithium dipping.

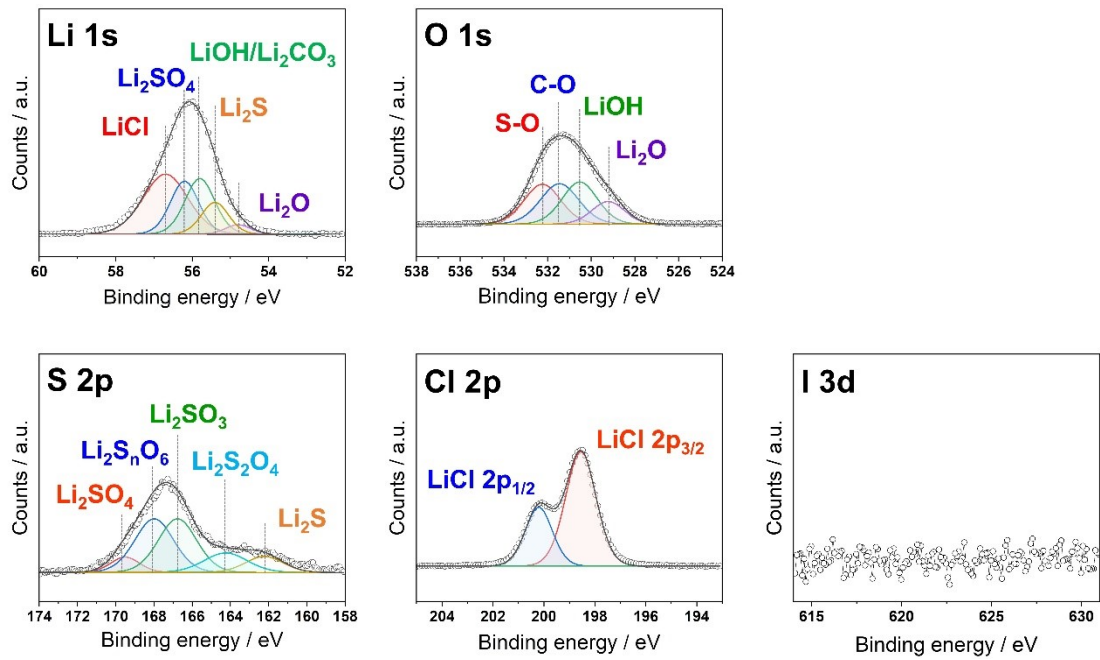


**Fig. S10.** XPS spectra of lithium metal after sequential surface treatment involving initial dipping in the pristine Li–SO<sub>2</sub> electrolyte followed by treatment in the I<sub>2</sub>–Li–SO<sub>2</sub> electrolyte.

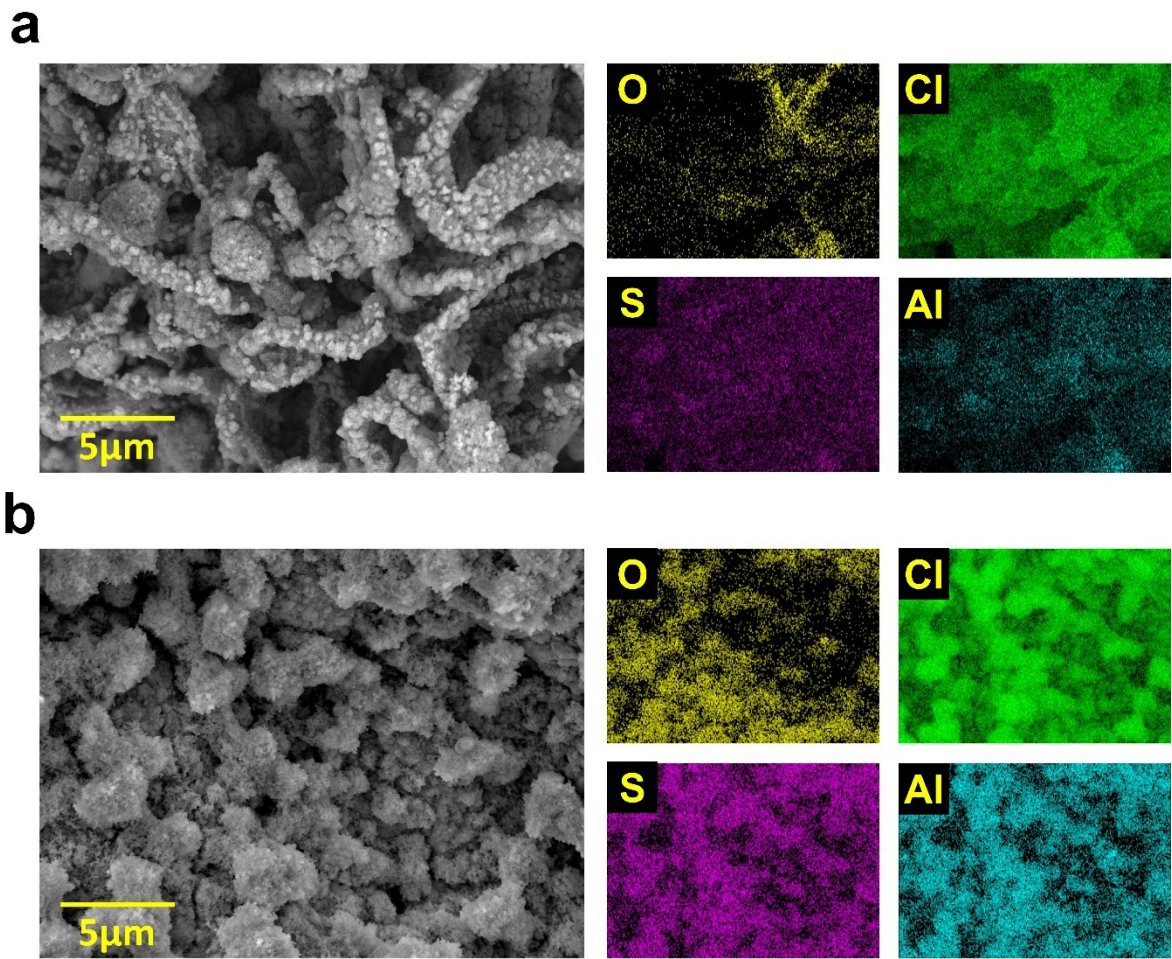


**Fig. S11.** SEM images and EDS elemental mapping of cycled lithium electrodes after Li//Li cycling at 3  $\text{mA cm}^{-2}$  and 5  $\text{mA h cm}^{-2}$  using (a) pristine lithium and (b)  $\text{I}_2$ -modified lithium. Corresponding EDS maps of O, S, Cl, and Al are shown to identify electrolyte-derived interphase products.

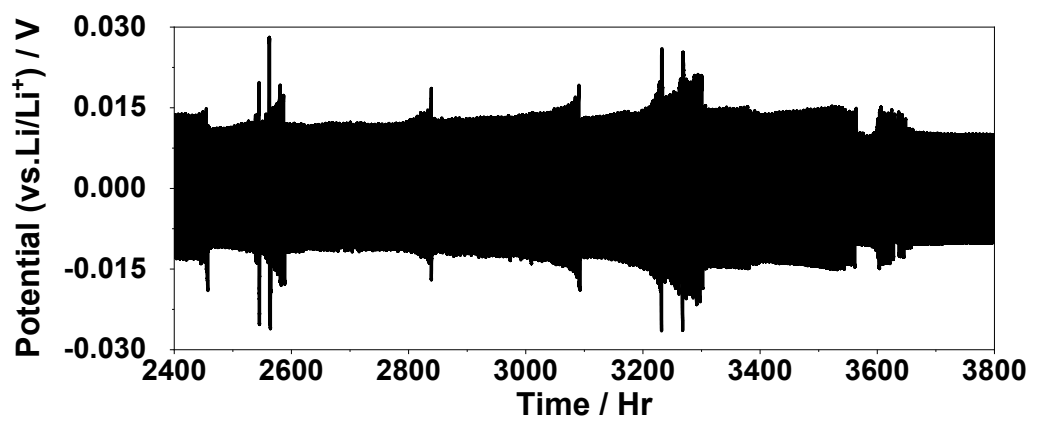


**Fig. S12.** Amplified electrochemical performance of Li//Li symmetric cells with pristine lithium electrode at current densities of  $1 \text{ mA cm}^{-2}$  with areal capacity of  $3 \text{ mA h cm}^{-2}$  during 400 cycles to 630 cycles.

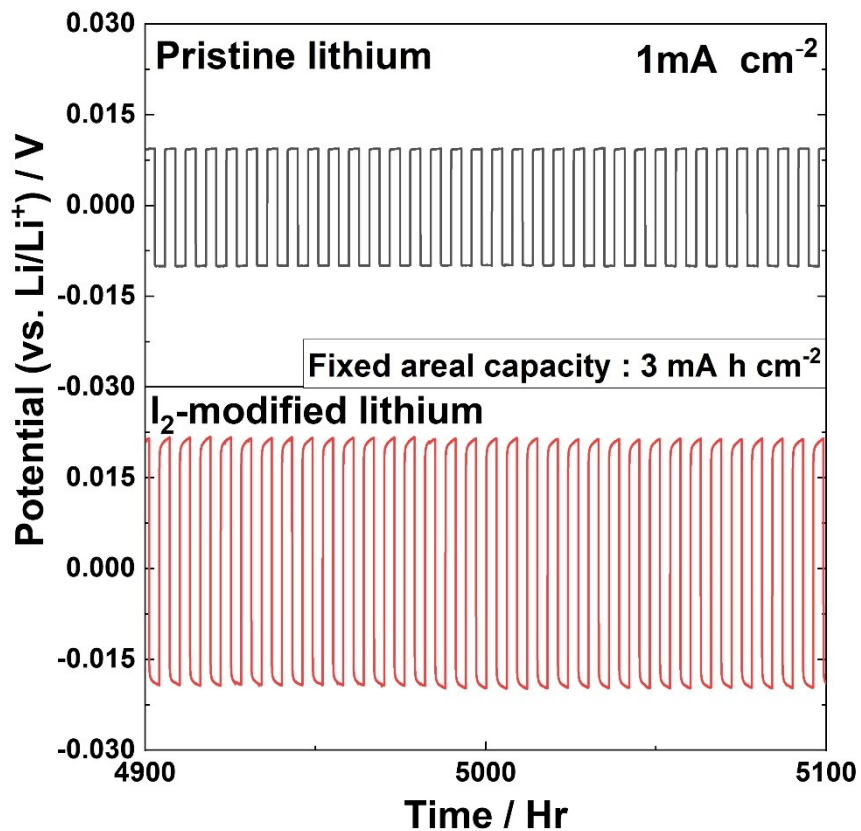


**Fig. S13.** Amplified electrochemical performance of Li//Li symmetric cells with pristine lithium electrode at current densities of  $1 \text{ mA cm}^{-2}$  with areal capacity of  $3 \text{ mA h cm}^{-2}$  during 400 cycles to 630 cycles.

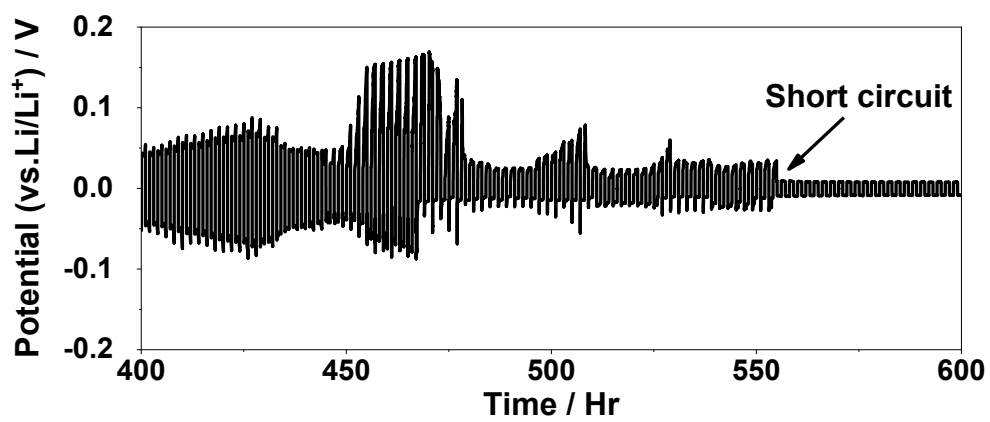


**Fig. S14.** Amplified electrochemical performance of  $\text{Li}/\text{Li}$  symmetric cells with pristine lithium electrode at current densities of  $3 \text{ mA cm}^{-2}$  with areal capacity of  $3 \text{ mA h cm}^{-2}$ .

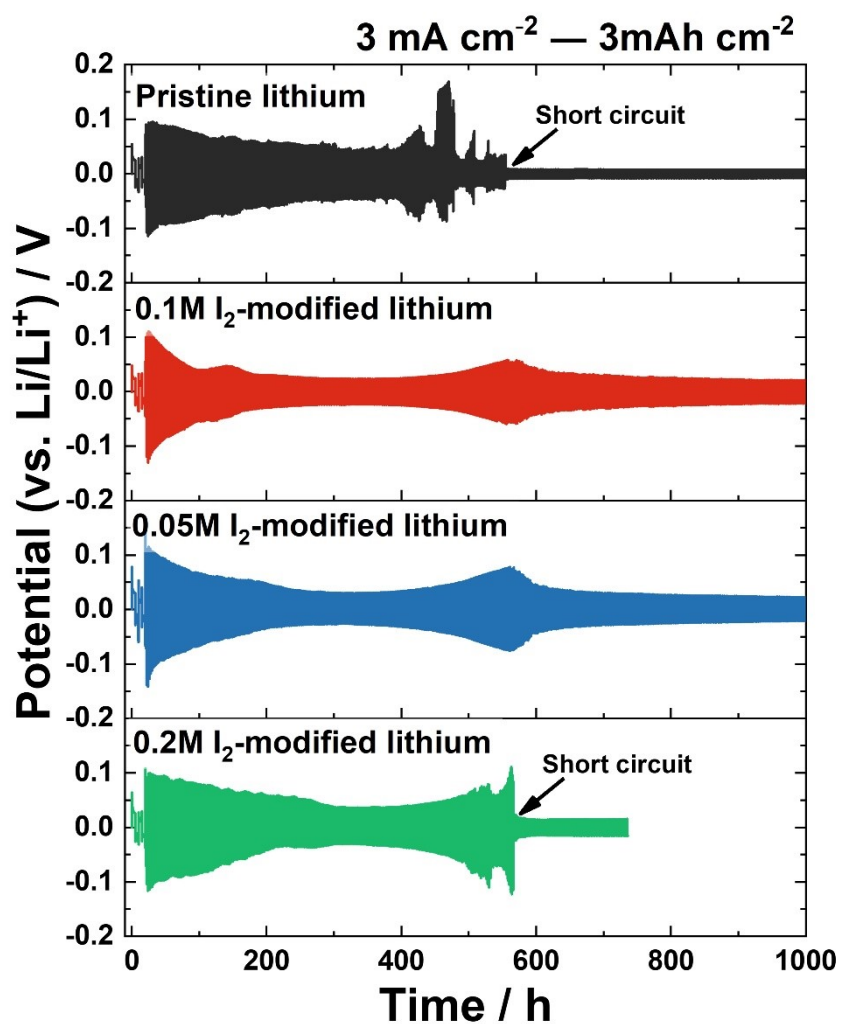


**Fig. S15.** Galvanostatic Li//Li symmetric-cell cycling profiles measured at  $3 \text{ mA cm}^{-2}$  with a fixed areal capacity of  $3 \text{ mA h cm}^{-2}$  for pristine lithium and modified Li electrodes using iodine-containing electrolytes with different  $\text{LiI}$  levels (0.05M, 0.10M, and 0.20M).

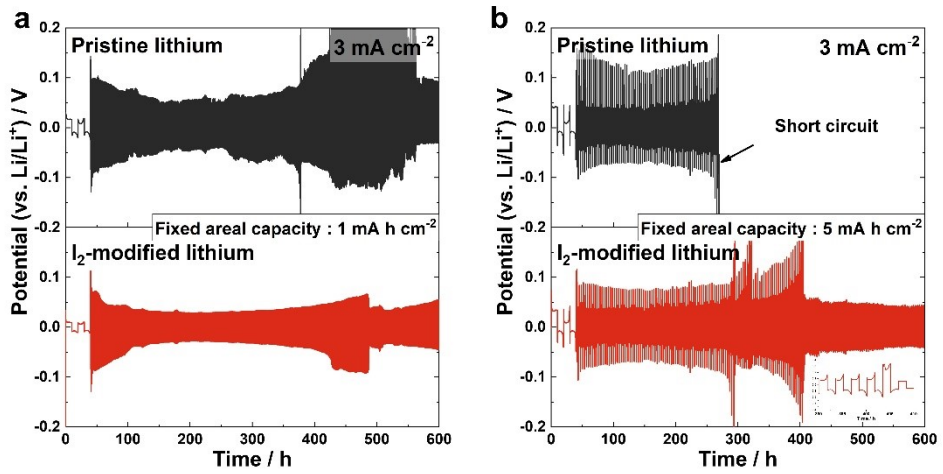


**Fig. S16.** Voltage profiles of Li symmetric cells using pristine lithium and  $I_2$ -modified lithium at a current density of  $3 \text{ mA cm}^{-2}$  with a fixed areal capacity of (a)  $1 \text{ mA h cm}^{-2}$  and (b)  $5 \text{ mA h cm}^{-2}$ .

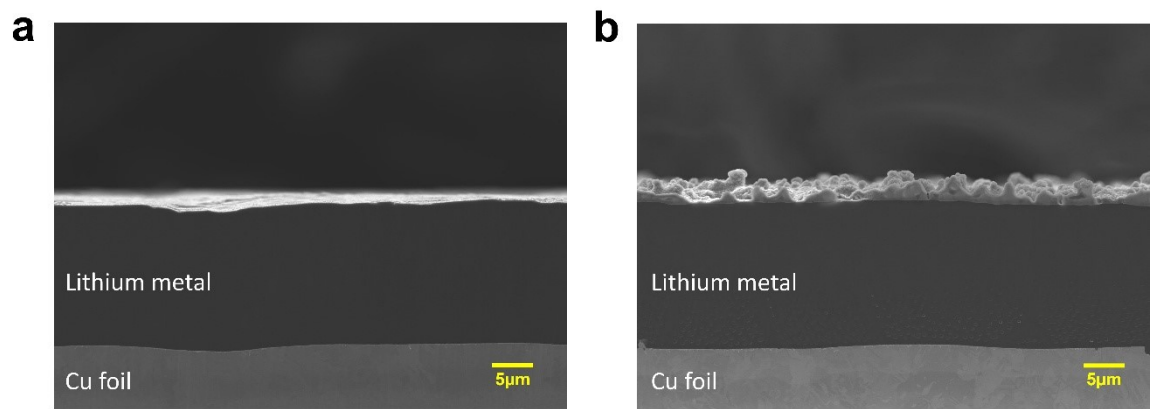


**Fig. S17.** Cross-sectional SEM images of thin lithium metal (18  $\mu\text{m}$ ) electrodes of (a) pristine lithium electrode and (b)  $\text{I}_2$ -modified lithium electrode.

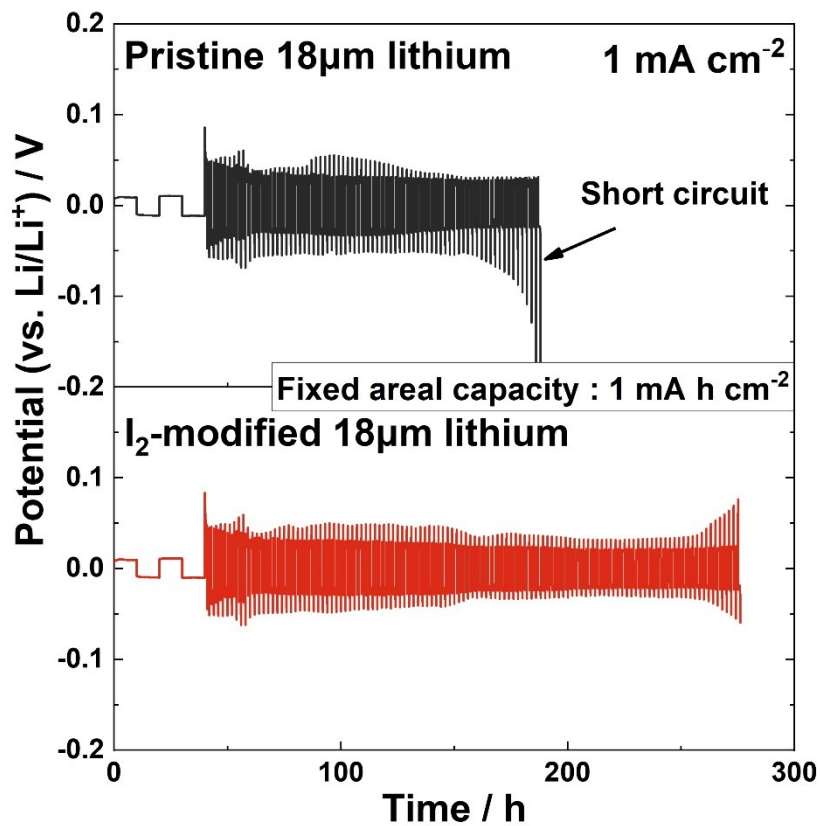


**Fig. S18.** Electrochemical performances of thin-lithium (18  $\mu$ m) Li//Li symmetric cells using pristine and I<sub>2</sub>-modified lithium at a current density of 1 mA cm $^{-2}$  with a fixed areal capacity of 1 mA h cm $^{-2}$ .

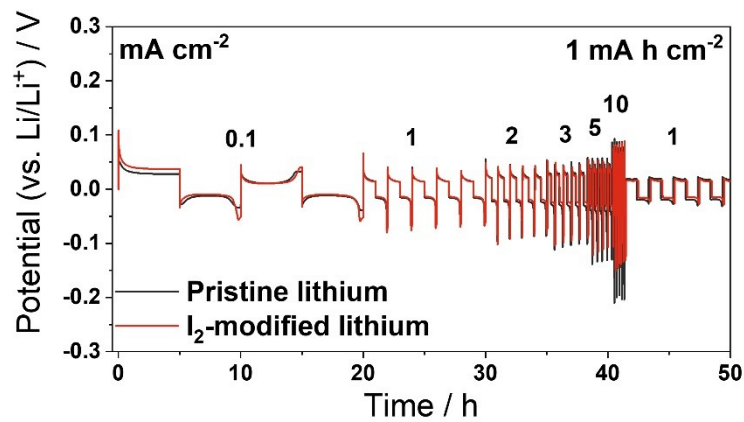


**Fig. S19.** Rate capability of Li//Li symmetric cells using pristine lithium and I<sub>2</sub>-modified lithium electrodes in the LiAlCl<sub>4</sub>–3SO<sub>2</sub> electrolyte. The cells were cycled at a fixed areal capacity of 1 mA h cm<sup>-2</sup> while the current density was sequentially increased from 0.1 to 10 mA cm<sup>-2</sup> and then returned to 1 mA cm<sup>-2</sup>.

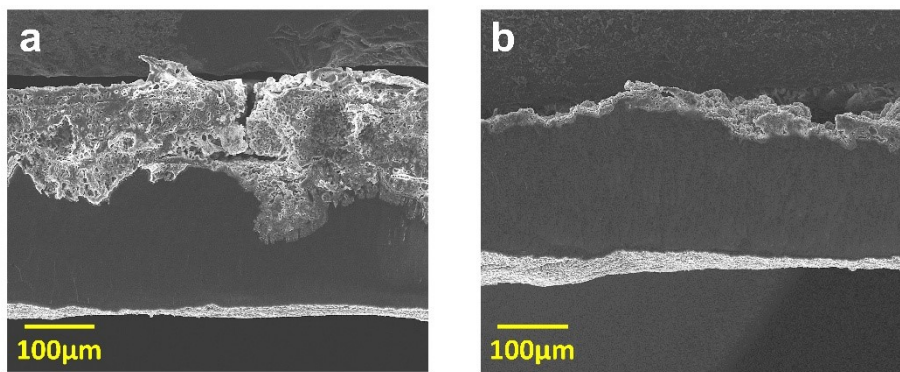


**Fig. S20.** Low-magnification cross-sectional SEM images of cycled lithium electrodes of (a) pristine lithium and (b) I<sub>2</sub>-modified lithium after 50 cycles.

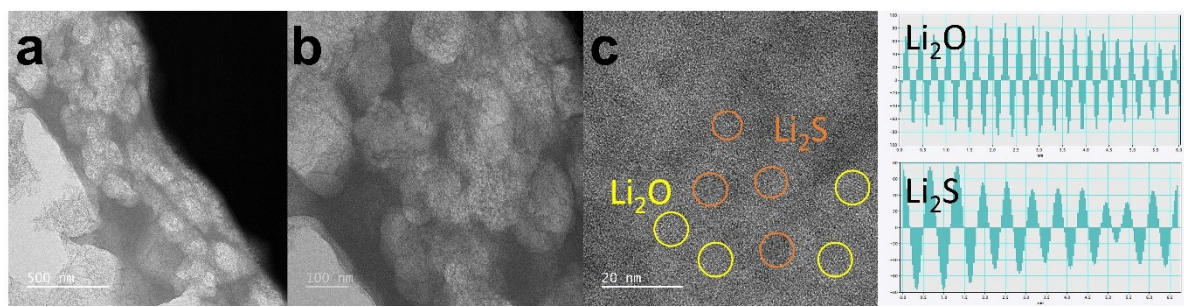


**Fig. S21.** TEM analysis of the I<sub>2</sub>-modified lithium metal electrode after 2 cycles. (a, b) Low- and (c) high-magnification TEM images with Interlayer d-spacing images of Li<sub>2</sub>O and Li<sub>2</sub>S, respectively.

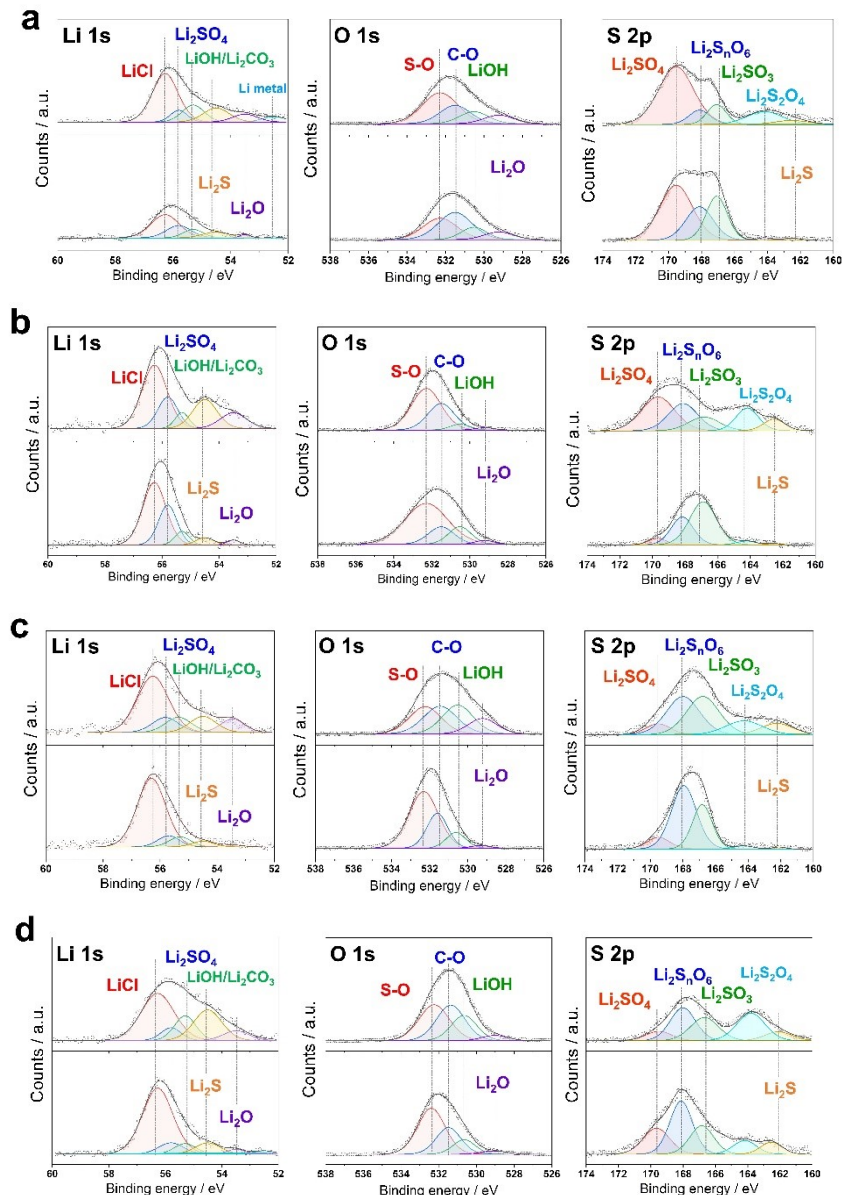


**Fig. S22.** Surface and depth-profiled XPS spectra of cycled lithium electrodes at different cycle numbers. XPS spectra of the Li 1s, O 1s, and S 2p regions collected from lithium electrodes after (a) 10, (b) 20, (c) 50, and (d) 100 cycles (upper for depth-profiled spectra after  $\text{Ar}^+$  sputtering for 120 sec, and the lower for the corresponding surface spectra).

	R1	R2	R3
<b>Pristine lithium</b>	<b>0.5 <math>\Omega</math></b>	<b>34.3 <math>\Omega</math></b>	<b>68.1 <math>\Omega</math></b>
<b>I<sub>2</sub>-modified lithium</b>	<b>0.8 <math>\Omega</math></b>	<b>41.9 <math>\Omega</math></b>	<b>320.7 <math>\Omega</math></b>

**Table S1.** Resistance values (R1, R2, R3) for symmetric Li//Li cells with pristine lithium and I<sub>2</sub>-modified lithium electrodes in LiAlCl<sub>4</sub>–3SO<sub>2</sub> electrolyte after 12 hours resting at open-circuit voltage. R1 represents the bulk electrolyte resistance, while R2 and R3 correspond to interfacial resistances of SEI and charge transfer processes, respectively.

		R1	R2	R3
<b>Pristine lithium</b>	<b>2 cycles</b>	<b>0.4 Ω</b>	<b>13.3 Ω</b>	<b>23.6 Ω</b>
	<b>10 cycles</b>	<b>0.5 Ω</b>	<b>17.5 Ω</b>	<b>28.4 Ω</b>
	<b>50 cycles</b>	<b>0.2 Ω</b>	<b>7.9 Ω</b>	<b>7.0 Ω</b>
<b>I<sub>2</sub>-modified lithium</b>	<b>2 cycles</b>	<b>0.6 Ω</b>	<b>41.9 Ω</b>	<b>69.5 Ω</b>
	<b>10 cycles</b>	<b>0.6 Ω</b>	<b>11.5 Ω</b>	<b>22.7 Ω</b>
	<b>50 cycles</b>	<b>0.3 Ω</b>	<b>8.5 Ω</b>	<b>10.8 Ω</b>

**Table S2.** Resistance values (R1, R2, R3) for symmetric Li//Li cells with pristine lithium and I<sub>2</sub>-modified lithium electrodes in LiAlCl<sub>4</sub>–3SO<sub>2</sub> electrolyte after 2 cycles, 10cycles, and 50 cycles. R1 represents the bulk electrolyte resistance, while R2 and R3 correspond to interfacial resistances of SEI and charge transfer processes, respectively.